Advances in Cement Research
Volume 25 Issue 3

Roles of water film thickness in fresh and hardened properties of mortar
Li, Chen and Kwan

Advances in Cement Research, 2013, **25**(3), 171–182
http://dx.doi.org/10.1680/adcr.12.00003
Paper 1200003
Received 05/01/2012; revised 02/05/2012; accepted 17/06/2012
Published online ahead of print 15/02/2013

ice
Institution of Civil Engineers
publishing

Roles of water film thickness in fresh and hardened properties of mortar

Yan Li
Department of Civil Engineering, The University of Hong Kong, Hong Kong

Jia Jian Chen
Department of Civil Engineering, The University of Hong Kong, Hong Kong

Albert K. H. Kwan
Department of Civil Engineering, The University of Hong Kong, Hong Kong

Supplementary cementitious materials (SCM) are commonly added to improve the performance of concrete. However, the effects of SCM on the behaviour of cement paste/mortar/concrete depend on many factors and have so far remained elusive, making the mix design of high-performance concrete containing SCM rather difficult. This paper evaluates the effects of SCM, the fresh and hardened properties of mortar made with superfine cement and condensed silica fume added at different water/cementitious materials ratios. First, the packing densities of the solid particles in the mortar samples were measured directly by a new wet packing method. Then, based on the measured packing densities, a mix parameter called water film thickness (WFT) was quantitatively evaluated. The results showed that the WFT plays important roles in the fresh and hardened properties of mortar, as demonstrated by the good correlations established between the WFT and the rheology as well as the strength of the mortar samples tested.

Introduction

The strength and durability of concrete can be greatly improved by lowering the water/cementitious materials (W/CM) ratio (Aïtcin, 1998). However, since the water added must be more than sufficient to fill the voids in the bulk volume of the cementitious materials, there is a limit to which the W/CM ratio can be lowered. Likewise, the dimensional stability of concrete can be enhanced and the cement consumption and 'carbon footprint' can be reduced by decreasing the cement paste volume (Kwan, 2003). However, as the cement paste volume must be more than sufficient to fill the voids in the bulk volume of the aggregate, there is also a limit to which the cement paste volume can be decreased. Hence, maximisation of particle packing density so as to reduce the volume of voids to be filled is the key to the production of high-performance concrete. For this purpose, the addition of supplementary cementitious materials (SCM) finer than cement to fill into the voids between cement grains is particularly effective. In fact, concrete produced with SCM added is often found to perform better in terms of workability, strength and durability (Aïtcin, 1998; Khatri *et al.*, 1995; Rizwan and Bier, 2009).

Although the use of SCM is already quite common, the effects of SCM are still not fully understood, as reflected by the widely different and even contradictory results reported by different researchers. Take condensed silica fume (CSF), which is considered one of the most effective SCM (FIP Commission on Concrete, 1988), as an example. Owing to its ultra-high fineness and high pozzolanic activity, the addition of CSF can significantly increase the concrete strength. However, the effects of CSF on the fresh properties of cement paste/mortar/concrete are relatively complicated and up to now no consensus has been reached. Kohno and Komatsu (1986) reported that at the same W/CM ratio, a mortar containing CSF would have a smaller flow compared with a plain mortar containing no CSF. However, Duval and Kadri (1998) demonstrated that cement replacement by CSF up to 10% by mass has no adverse effect on concrete workability. Similarly, Zhang and Han (2000) showed that the yield stress and viscosity of a cement paste could be decreased by adding CSF to replace 10% by mass of cement. More recently, Artelt and Garcia (2008) examined several mortar mixes with and without CSF and concluded that the presence of CSF would impair the flowability as evidenced by the smaller flow spread and longer flow time obtained for the CSF mortars.

The authors are of the view that the addition of fine SCM has two major effects and it is the combined action of these that governs the rheology of cement paste/mortar/concrete. First, the fine SCM particles would fill into the voids between cement grains to increase the packing density of the particle system. As a result, the volume of voids would decrease and the amount of water in excess of that needed to fill the voids (i.e. the amount of excess water) for forming water films coating the solid particles would increase. Such an effect is beneficial to the flowability of the water–solid mixture. Another effect is that with fine SCM added, the total surface area of the solid particles would increase so that with the same amount of excess water available, the average thickness of the water films coating the solid particles would decrease. This is in agreement with Claisse *et al.* (2001), who pointed out that the specific surface area of the solid particles has a great influence on the rheology of cement paste, and Ferraris *et al.* (2001), who suggested that the increase in packing density and the increase in solid surface area have opposite effects on the rheology of cement paste. Consequently, the net influence of adding fine SCM is dependent on the relative magnitudes of the two opposite effects.

Dating back to the 1960s, Powers (1968) proposed that it is the excess paste (paste in excess of that needed to fill the voids between aggregate particles) that gives the mortar or concrete workability. Similarly, Helmuth (1980) suggested that it is the excess water (water in excess of that needed to fill the voids between cement grains) that forms water films coating the cement grains and it should be the thickness of the water films that governs the consistence of cement paste. Zhang *et al.* (1996) found that the addition of fine pozzolanic material could increase the packing density and thereby decrease the amount of filling water in the voids and increase the amount of excess water in the surface layers. Later, Kwan and his research team (Kwan and Wong, 2008; Wong and Kwan, 2008a) proposed that the average water film thickness (WFT) may be evaluated indirectly as the excess water to solid surface area ratio. Hence, by measuring the packing density and solid surface area of the solid particles, the WFT can be determined without direct measurement.

However, the packing density of fine solid particles is not easy to measure, because of agglomeration caused by the presence of inter-particle forces (Yu *et al.*, 1997). The existing dry packing methods of measuring packing density under dry conditions have the major problems that the measured results are sensitive to the amount of compaction applied (Svarovsky, 1987), and that they cannot take into account the effects of water and superplasticiser (SP), which have significant effects on the packing density. Without accurate measurement of packing density, it is impossible to determine precisely the WFT for investigating the effects of WFT. In other words, the lack of a proper method for measuring the packing density of fine solid particles has been the main hurdle in the study of WFT.

Recently, the authors' research team has developed a wet packing method for direct measurement of the packing densities of cementitious materials (Wong and Kwan, 2008b), fine aggregate (Fung *et al.*, 2009) and cementitious materials plus fine aggregate (Kwan and Fung, 2009), and by comparing with theoretical results based on existing packing models, verified the accuracy and applicability of this wet packing method (Kwan and Fung, 2009; Wong and Kwan, 2008c). With the packing density directly measured and then the WFT determined as the excess water to solid surface area ratio, the authors' research team has demonstrated that the WFT is the single most important parameter governing the rheology of cement paste (Kwan and Wong, 2008; Wong and Kwan, 2008a).

Herein, a comprehensive testing programme was carried out to study the roles of WFT in mortar mixes containing triple-blended cementitious materials. To maximise the packing density of the cementitious materials, superfine cement (SFC), which was finer than cement, was added to fill the voids between the cement grains, and CSF, which had the highest fineness, was added to fill the voids between the other cementitious materials. A number of mortar samples with different SFC and CSF contents and different W/CM ratios were made for packing density, rheology, adhesiveness and strength measurements. From the test results, the rheological properties, adhesiveness and strength of the mortar samples were correlated to the WFT for in-depth analysis of the roles of WFT in the fresh and hardened properties of mortar.

Experimental programme

To study the roles of WFT in fresh and hardened properties of mortar, an experimental programme was carried out. Three different SFC contents, namely 0%, 10% and 20%, and two different CSF contents, namely 0% and 10%, each expressed as a percentage by volume of the total cementitious materials, were adopted for the design of the mortar samples. To exclude the effect of variation in fine aggregate content, the total cementitious materials to fine aggregate ratio was fixed at 0·75 by volume. The W/CM ratio by volume was varied from 0·5 to 1·2. In total, 27 mortar samples were produced for testing. The mix proportions of the mortar samples are summarised in Table 1. Each mortar sample is assigned a designation of M-X-Y-Z, where M denotes mortar, X and Y denote the SFC and CSF contents, respectively, and Z denotes the W/CM ratio by volume. For reference, the W/CM ratio by mass of each mortar sample is listed in the second column of Table 1.

A SP was added to each mortar sample. As SP is a surface reactant and it is the SP dosage per solid surface area that actually governs the effectiveness of the SP (Kwan *et al.*, 2012; Wong and Kwan, 2008a), the SP dosage was determined according to the total surface area of the solid particles in the mortar. Before setting the SP dosage to be used, trial cement paste mixing using different SP dosages was carried out and it was found that the saturation dosage (the dosage beyond which further addition of the SP yields little further increase in flowability) was $2{\cdot}6 \times 10^{-7}$ kg/m^2 of the solid surface area. Hence, the SP dosage in terms of liquid mass of SP per solid surface area was set at $2{\cdot}6 \times 10^{-7}$ kg/m^2 for all the mortar samples. It is noteworthy that as SFC and CSF have higher fineness, the SP dosage per mass of cementitious materials was higher at higher SFC and/or CSF contents.

The experimental programme consisted of three parts. The first part was to measure the packing density of the solid particles in

Mix no.	W/CM ratio by mass	Dosage of each ingredient in the mortar: kg/m^3						Packing density (voids ratio)	WFT: μm
		OPC	SFC	CSF	FA	Water	SP		
M-0-0-0·6	0·193	1048	0	0	1099	205	12	0·737	−0·163
M-0-0-0·8	0·257	982	0	0	1030	256	11	(0·357)	−0·019
M-0-0-1·0	0·321	924	0	0	969	300	11		0·125
M-0-0-1·2	0·386	872	0	0	914	339	10		0·269
M-10-0-0·6	0·194	943	99	0	1098	204	13	0·749	−0·117
M-10-0-0·8	0·259	883	93	0	1029	255	12	(0·335)	0·016
M-10-0-1·0	0·323	831	87	0	968	299	12		0·149
M-10-0-1·2	0·388	784	82	0	914	338	11		0·282
M-20-0-0·6	0·195	837	198	0	1097	203	14	0·755	−0·094
M-20-0-0·8	0·260	784	185	0	1028	254	13	(0·325)	0·030
M-20-0-1·0	0·325	738	174	0	967	298	12		0·153
M-20-0-1·2	0·390	697	165	0	913	337	12		0·277
M-0-10-0·5	0·166	966	0	76	1126	167	23	0·780	−0·059
M-0-10-0·6	0·199	934	0	73	1088	195	22	(0·282)	−0·021
M-0-10-0·8	0·265	876	0	69	1020	245	21		0·057
M-0-10-1·0	0·331	824	0	65	960	290	20		0·134
M-0-10-1·2	0·397	778	0	61	907	329	19		0·211
M-10-10-0·5	0·167	858	101	76	1124	166	24	0·789	−0·036
M-10-10-0·6	0·200	829	98	73	1087	194	23	(0·267)	0·001
M-10-10-0·8	0·267	778	92	69	1019	244	22		0·075
M-10-10-1·0	0·333	732	86	65	959	289	21		0·149
M-10-10-1·2	0·400	691	82	61	906	328	20		0·222
M-20-10-0·5	0·168	750	202	76	1123	165	25	0·800	−0·028
M-20-10-0·6	0·201	725	196	73	1086	193	24	(0·250)	0·007
M-20-10-0·8	0·268	680	183	69	1018	243	23		0·078
M-20-10-1·0	0·335	640	173	65	958	288	22		0·149
M-20-10-1·2	0·402	604	163	61	905	327	20		0·220

FA, fine aggregate

Table 1. Mix proportions, packing density and WFT

each mortar sample by a wet packing method developed by the authors' research team. In the second and third parts, the fresh and hardened properties of mortar samples were measured. Each mortar sample was produced using a standard mixer by first adding all the water and SP to the mixer and then adding the solid materials bit by bit to the mixer while mixing. This mixing procedure has been found to be more effective than the conventional mixing procedure of adding all the water and solid materials to the mixer in one single batch, especially when the water content is low and/or ultrafine filler is added (Wong and Kwan, 2008b). All of the mixing and testing procedures were carried out in a laboratory maintained at a temperature of 24 ± 2°C.

Materials

The cement used was an ordinary Portland cement (OPC) obtained from the local market. It was of strength class 52·5N and had been tested to comply with BS EN 197-1:2000 (BSI, 2000). The SFC and CSF used were imported from Europe. According to the supplier, the SFC was a slag-cement containing 80% slag and 20% cement. On the other hand, the CSF had been tested by the supplier to comply with ASTM C 1240-03 (ASTM, 2003). The fine aggregate used was a local crushed granite rock fine with a maximum size of 1·18 mm and a water absorption of 1·6% by mass. The relative densities of the OPC, SFC, CSF and fine aggregate had been measured in accordance with BS EN 196-6: 2010 (BSI, 2010) as 3·11, 2·94, 2·20 and 2·48, respectively. A laser diffraction particle size analyser was used to measure the particle size distributions of the materials and the results are plotted in Figure 1. Based on their particle size distributions, the specific surface areas of the OPC, SFC, CSF and fine aggregate were calculated as $1{\cdot}12 \times 10^6$ m^2/m^3, $2{\cdot}29 \times 10^6$ m^2/m^3, $1{\cdot}33 \times 10^7$ m^2/m^3 and $2{\cdot}1 \times 10^5$ m^2/m^3, respectively. The SP employed was a polycarboxylate-based

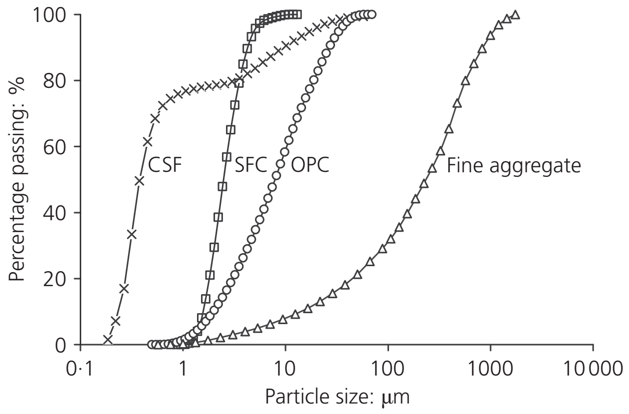

Figure 1. Particle size distributions of CSF, SFC, OPC and fine aggregate

type with a solid mass content of 20% and a relative density of 1·03.

Determination of packing density and WFT

The packing density of the particle system comprising the OPC, SFC, CSF and fine aggregate was measured by a wet packing method with the solid particles mixed with water so that the solid particles were under wet conditions. Details of the wet packing method have been presented before (Kwan and Fung, 2009; Wong and Kwan, 2008b). Basically, the wet packing method determines the packing density of the solid particles in a mortar as the maximum solid concentration of the solid particles that can be achieved at different water/solid (W/S) ratios by volume.

Based on the packing density result, the voids ratio of the particle system may be determined as

$$u = \frac{1 - \phi_{\max}}{\phi_{\max}} \tag{1}$$

where u is the voids ratio (the ratio of the volume of voids in the bulk volume to the solid volume of the solid particles) and $\phi_{\max}$ is the maximum solid concentration of the solid particles. From the voids ratio so determined, the excess water ratio of the mortar can be evaluated as

$$u'_{\mathrm{w}} = u_{\mathrm{w}} - u \tag{2}$$

where u'_{w} is the excess water ratio and u_{w} is the water ratio (same as the W/S ratio by volume) of the mortar. This excess water ratio has the physical meaning of being the amount of excess water in the mortar per solid volume of the particles. Meanwhile, the specific surface area (defined as solid surface area per unit solid volume) in the mortar A_M can be calculated as

$$A_{\mathrm{M}} = A_{\mathrm{OPC}} \times R_{\mathrm{OPC}} + A_{\mathrm{SFC}} \times R_{\mathrm{SFC}} + A_{\mathrm{CSF}} \times R_{\mathrm{CSF}} + A_{\mathrm{FA}} \times R_{\mathrm{FA}} \tag{3}$$

in which A_{OPC}, A_{SFC}, A_{CSF} and A_{FA} are, respectively, the specific surface areas of OPC, SFC, CSF and fine aggregate, while R_{OPC}, R_{SFC}, R_{CSF} and R_{FA} are, respectively, the volumetric ratios of OPC, SFC, CSF and fine aggregate to the total solid volume. With the values of u'_{w} and A_{M} so obtained, the WFT may be calculated as

$$\mathrm{WFT} = \frac{u'_{\mathrm{w}}}{A_{\mathrm{M}}} \tag{4}$$

Measurement of flow spread and flow rate

The mini slump cone test and mini V-funnel test were used to measure the flow spread and flow rate of the mortar samples, respectively. Both the mini slump cone and mini V-funnel tests for mortar may be regarded as reduced scale versions of the slump and V-funnel tests for concrete. There are several versions of mini slump cone and mini V-funnel with different dimensions. The versions adopted here are the same as those used by Okamura and Ouchi (2003). The detailed test procedures have been given elsewhere (Kwan *et al.*, 2010).

Measurement of yield stress and apparent viscosity

The shear vane test was used to evaluate the rheological properties of the mortar samples. It was carried out using a speed-controlled rheometer equipped with a shear vane, measuring 20 mm wide and 40 mm long, and a cylindrical container, having an inner diameter of 40 mm. The inner wall of the container was profiled with grooves of which the asperity was larger than the largest particle in the mortar to minimise slippage of the mortar during shearing. Since the details have been given before (Kwan *et al.*, 2010), only the basic features are presented here.

At the onset of the test, the shear vane was concentrically inserted into the mortar sample in the cylindrical container and then set to rotate at controlled rotation speed, following a shearing sequence that consisted of two shearing cycles. The first shearing cycle, called the pre-shearing cycle, was to ensure all the samples tested had undergone the same shearing history before measurement. The second shearing cycle, called the data-logging cycle, was the cycle in which actual measurement was carried out. In each shearing cycle, the shear rate was increased from 0 to 14 s^{-1} in 75 s and then decreased from 14 to 0 s^{-1} in another 75 s. The shear stress–shear rate curves obtained at decreasing shear rate, which is generally more consistent and repeatable, were used for evaluating the rheological properties of the mortar sample. For each mortar sample, the best-fit curve based on the Herschel–Bulkley model was derived by regression analysis. From the best-fit curve so obtained, the shear stress at a shear rate of 0 s^{-1} and the ratio of shear stress to shear rate at a shear rate of 14 s^{-1} were taken as the yield stress and the apparent viscosity, respectively.

Measurement of adhesiveness

There is, up to now, no established test method for measuring the adhesiveness of mortar. Herein, a new test, called the stone rod adhesion test, was developed. The apparatus, shown in Figure 2, consists of a handle with six stone rods vertically fixed underneath and a container. The stone rods are made of granite, which is a commonly used rock for coarse aggregate, and each stone rod has a diameter of 10 mm and an exposed length of 110 mm. Before the test, the stone rods were immersed in water for at least 24 h and then wiped clean by a piece of dry cloth so that the stone rods were 'saturated and surface dry'. During the test, the stone rods were immersed into the mortar inside the container with an immersion depth of 100 mm, as indicated by the mortar surface reaching the 100 mm mark on the stone rods. The stone rods were left immersed in the mortar for 1 min and afterwards pulled out steadily and slowly. The handle holding the stone rods was then placed on a stand to allow dripping to take place. After several minutes when no more dripping occurred, the increase in weight of the handle (in other words, the weight of mortar adhering to the stone rods) was measured and taken as the adhesiveness of the mortar tested.

Measurement of cube strength

Three 100 mm cubes were made from each mortar sample. The cubes were each made by placing the mortar into a cube mould, inserting a vibrator into the mortar for compaction and covering the top surface of the mould with a plastic sheet. The cubes were then stored at a temperature of 24 ± 2°C. After one day, the moulds were removed and the cubes were cured in water at a temperature of 27 ± 2°C. All the three cubes were tested at the age of 28 days.

Experimental results

Packing density and water film thickness

The measured packing densities of the mortar mixes are tabulated in the ninth column of Table 1. It can be seen from these results that without the addition of any SFC or CSF, the solid mix of OPC and fine aggregate was measured to have a packing density of 0·737. With SFC but no CSF added, the packing density was increased to 0·749 at 10% SFC content and to 0·755 at 20% SFC content. With CSF but no SFC added, the packing density was increased to 0·780 at 10% CSF content. This demonstrates that the SFC and CSF, when added individually, could effectively increase the packing density of the solid particles in mortar. Compared to the SFC, the CSF was more effective due to its higher fineness.

The results also show that with both SFC and CSF added, the packing density of the solid particles could be further increased. With 10% CSF added, the packing density was increased by 5·8% from 0·737 to 0·780, by 5·3% from 0·749 to 0·789, and by 6·0% from 0·755 to 0·800 at 0%, 10% and 20% SFC contents, respectively. Hence, regardless of the SFC content, the addition of 10% CSF would increase the packing density by about 5·3% to 6·0%. On the other hand, with 20% SFC added, the packing

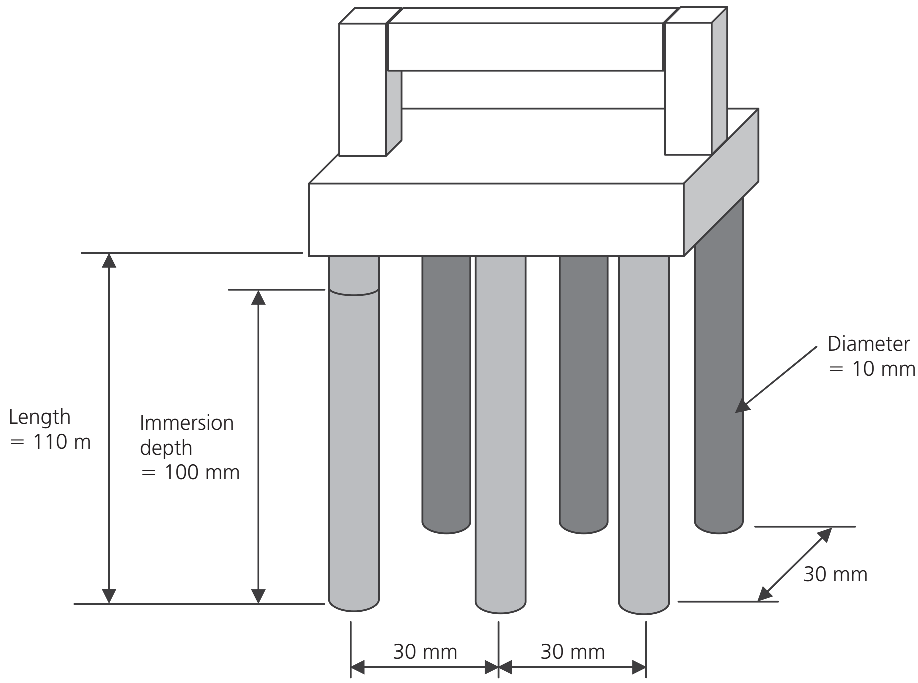

Figure 2. Details of apparatus for stone rod adhesion test

density was increased by 2·4% from 0·737 to 0·755 and by 2·6% from 0·780 to 0·800 at 0% and 10% CSF contents, respectively. Hence, regardless of the CSF content, the addition of 20% SFC would increase the packing density by about 2·4% to 2·6%. Overall, it is evident that blending OPC with both SFC and CSF so that the voids between cement grains are successively filled by finer and even finer particles is a more effective way of increasing the packing density than just blending OPC with SFC or just blending OPC with CSF.

The voids ratios of the solid particles, as calculated by Equation 1, are also tabulated in the ninth column of Table 1. It can be seen that a single addition of 20% SFC decreased the voids ratio from 0·357 to 0·325, a single addition of 10% CSF decreased the voids ratio from 0·357 to 0·282, whereas the joint addition of 20% SFC and 10% CSF decreased the voids ratio from 0·357 to 0·250. Compared to the maximum increase in packing density of 8·5%, which appears small, the corresponding decrease in voids ratio of 30·0% is quite substantial. Such a reduction in voids ratio due to the addition of fine SCM would decrease the amount of water needed to fill the voids between the solid particles so as to increase the amount of excess water available for forming water films coating the solid particles in the mortar.

The WFT of the mortar mixes are listed in the last column of Table 1 and plotted against the W/S ratios for different SFC and CSF contents in Figure 3. From the figure, it can be seen that at W/S ratio $\leqslant 0·45$ (corresponding W/CM ratio by mass $\leqslant 0·32$), the addition of SFC and/or CSF would significantly increase the WFT. However, at higher W/S ratio, the addition of SFC would slightly increase the WFT but the addition of CSF would significantly decrease the WFT. This phenomenon can be explained by Equation 4, which stipulates that the WFT is determined by both the excess water ratio and the total solid surface area. Generally, the proportional increase in excess water ratio owing to the addition of a SCM finer than cement is larger at lower W/S ratio and smaller at higher W/S ratio, whereas the proportional increase in total solid surface area is larger when the SCM has higher fineness and smaller when the SCM has lower fineness. If the proportional increase in excess water ratio were larger than the proportional increase in total solid surface area, the WFT would increase, otherwise, the WFT would decrease.

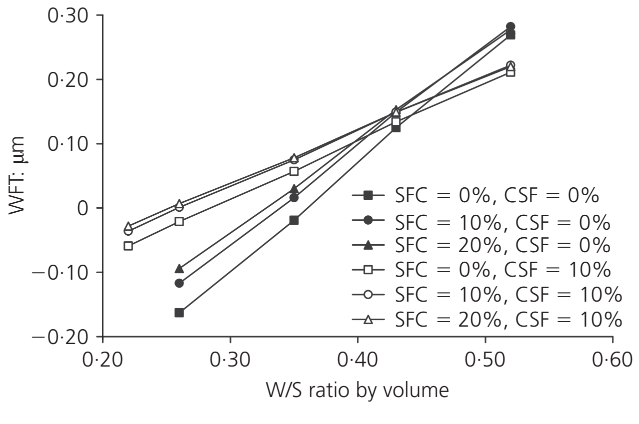

Figure 3. Variation of WFT with W/S ratio at different SFC and CSF contents

From the above results, it is evident that the SFC, which is finer than cement but not as fine as CSF, is effective in increasing the WFT over a wider range of water content but is not as effective as CSF at low water content. On the other hand, the much finer CSF, which produces larger increases in packing density and total solid surface area when added, is more effective than SFC in increasing the WFT but only at low water content. Hence, the suitable amounts of SFC and CSF to be added to increase the WFT are dependent on the water content.

Flow spread and flow rate

The flow spread and flow rate results are tabulated in the second and third columns of Table 2 and plotted against the W/S ratio in Figure 4. As expected, both the flow spread and flow rate generally increased with the W/S ratio. However, the effects of SFC and CSF appeared to be fairly complicated. At W/S ratio $\leqslant 0·45$, the addition of SFC and/or CSF significantly increased the flow spread and flow rate, but at W/S ratio $> 0·45$, the addition of SFC and/or CSF did not always increase the flow spread and flow rate. Relatively, the CSF has greater effects on the flowability than the SFC because of its larger effects on the WFT. Overall, as depicted by the widely spaced flowability–W/S ratio curves for mortar mixes containing different blends of SCM, it may be said that the flowability of mortar is dependent not only on the W/S ratio, but also on the solid ingredient contents in the mortar.

Yield stress and apparent viscosity

The yield stress and apparent viscosity results are tabulated in the fourth and fifth columns of Table 2 and plotted against the W/S ratio in Figure 5. At low W/S ratio, the torque required to shear the mortar sample had occasionally exceeded the capacity of the rheometer causing the yield stress and apparent viscosity of some mortar mixes to be undetermined (each shown in Table 2 by a dash). From the curves plotted, it can be seen that both these two rheological properties decreased as the W/S ratio increased and that the effects of SFC and CSF were generally more significant at lower W/S ratio. On the whole, both rheological properties varied more notably with the CSF content than with the SFC content, as illustrated by the widely spaced curves plotted for different CSF contents, which are obviously divided into two series: one series with no CSF added and the other series with 10% CSF added. Hence, the rheological properties of mortar are governed not only by the water content but also by the solid ingredient contents in the mortar.

Adhesiveness

The stone rod adhesion test results are tabulated in the sixth column of Table 2 and plotted against the W/S ratio in Figure 6. It is evident that generally the adhesiveness varied with the W/S

Mix no.	Flow spread: mm	Flow rate: ml/s	Yield stress: Pa	Apparent viscosity: Pas	Adhesiveness: g	28-Day cube strength: MPa
M-0-0-0·6	0·0	0·0	—	—	0·0	7·0
M-0-0-0·8	5·5	0·0	—	—	0·6	90·8
M-0-0-1·0	155·0	169·8	9·2	6·7	26·0	91·4
M-0-0-1·2	210·0	365·8	2·6	3·1	13·4	72·9
M-10-0-0·6	0·0	0·0	—	—	0·0	84·8
M-10-0-0·8	1·5	0·0	95·8	36·2	2·7	95·8
M-10-0-1·0	195·0	202·5	3·8	2·9	19·8	95·9
M-10-0-1·2	206·0	391·3	2·8	2·6	15·9	82·1
M-20-0-0·6	0·0	0·0	—	—	0·0	88·8
M-20-0-0·8	0·0	8·5	78·3	29·2	93·3	99·8
M-20-0-1·0	191·0	226·8	5·2	4·0	15·8	95·5
M-20-0-1·2	195·0	354·4	2·7	1·7	12·8	90·0
M-0-10-0·5	0·0	0·0	—	—	0·0	98·6
M-0-10-0·6	0·0	0·0	—	—	0·0	117·6
M-0-10-0·8	162·0	69·8	8·2	9·7	24·0	105·9
M-0-10-1·0	260·5	236·3	2·5	2·5	12·8	99·1
M-0-10-1·2	289·5	365·8	1·2	1·3	9·6	89·1
M-10-10-0·5	0·0	0·0	—	—	0·0	109·1
M-10-10-0·6	2·5	0·0	—	—	0·6	116·6
M-10-10-0·8	171·5	97·8	6·0	7·4	23·8	108·2
M-10-10-1·0	250·0	252	2·7	2·8	9·4	100·7
M-10-10-1·2	274·0	354·4	1·6	1·8	9·0	91·0
M-20-10-0·5	0·0	0·0	—	—	0·0	87·2
M-20-10-0·6	0·0	2·9	59·2	46·9	103·6	116·0
M-20-10-0·8	191·5	155·3	5·9	5·5	26·0	112·9
M-20-10-1·0	230·5	315·0	2·6	2·9	22·6	105·9
M-20-10-1·2	246·0	365·8	2·1	2·2	13·2	96·3

Table 2. Flowability, rheological properties, adhesiveness and strength

ratio in such a way that when the W/S ratio was low, the adhesiveness increased as the W/S ratio increased, but after reaching a certain peak value, the adhesiveness decreased as the W/S ratio increased further. This implies that the water added to a mortar may have a positive or negative effect on the adhesiveness and there exists an optimum water content depending on the mix proportions of the solid ingredients for maximum adhesiveness.

Cube strength

The cube strength results are tabulated in the last column of Table 2. Each cube strength result presented is the average of the three cubes cast and tested at the same time. Generally, the cube strength varied with the W/CM ratio in such a way that as the W/CM ratio decreased starting from a relatively high value, the strength increased until a certain peak value was reached and then as the W/CM ratio decreased further, the strength started to decrease. This was because while the W/CM ratio was still high, the water was more than sufficient to fill the voids and in such a case, as usual, the strength increased as the W/CM ratio decreased. However, when the W/CM ratio decreased to such a level that the water was no longer sufficient to fill the voids, air was entrapped inside the voids, causing the strength to decrease.

In this case, with no SCM added, the maximum cube strength achieved was 91·4 MPa. With 10% SFC added, the maximum cube strength was increased to 95·9 MPa. With 10% CSF added, the maximum cube strength was increased to 117·6 MPa. With 10% SFC and 10% CSF added together, the maximum cube strength achieved was 116·6 MPa. These results show that the addition of CSF has a great effect on the strength, whereas the addition of SFC has little effect especially after CSF has been added. It is noteworthy that the optimum W/CM ratio for maximum strength was lower at higher SFC and CSF contents.

Roles of water film thickness

From the above, it is evident that the addition of SCM finer than cement has significant effects on the packing density, solid surface area and WFT, which in turn govern the fresh and hardened properties of mortar. The effects of SCM on the

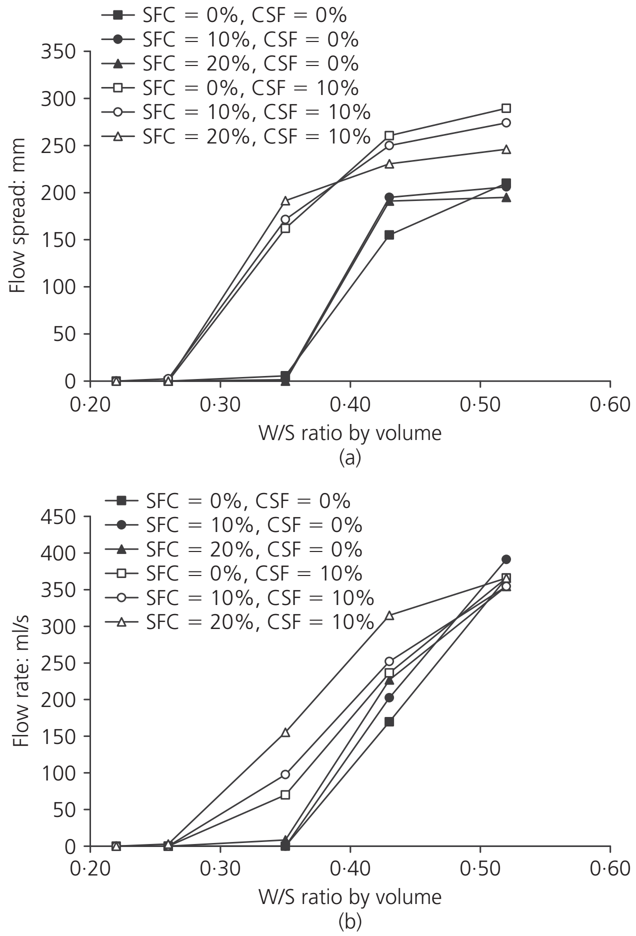

Figure 4. Flowability against W/S ratio

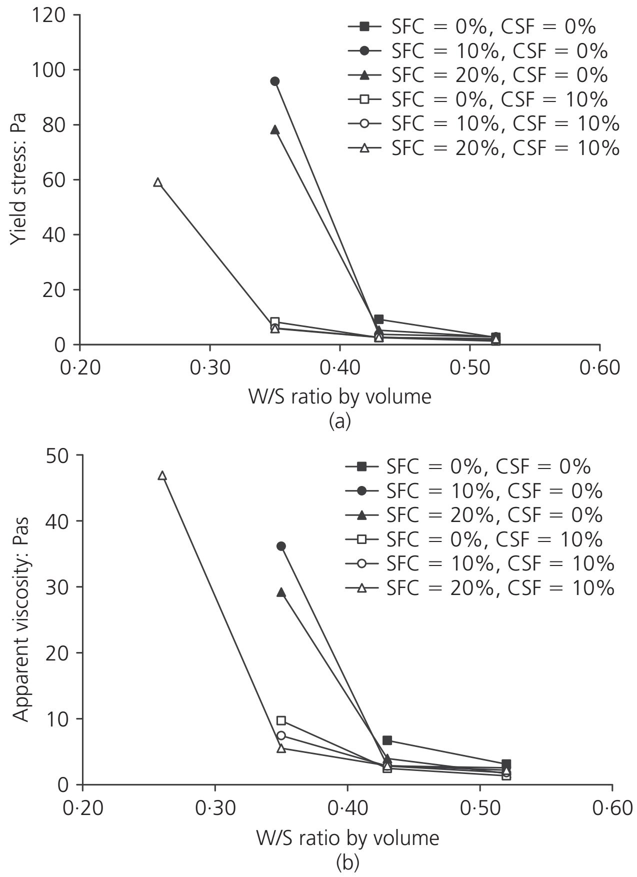

Figure 5. Rheological properties against W/S ratio

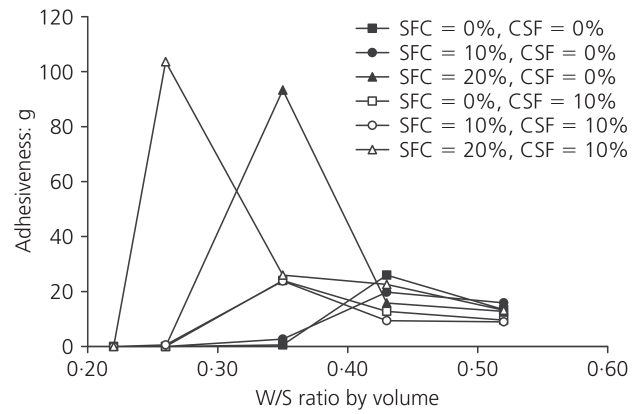

Figure 6. Adhesiveness against W/S ratio

packing density and solid surface area are not dependent on the W/S ratio, but the effects of SCM on the WFT are dependent on the W/S ratio. For this reason, the net effects of SCM on the properties of mortar could vary with the water content. Herein, it is suggested that the combined effects of the SCM content and W/S ratio should be evaluated in terms of the WFT.

The WFT of the mortar samples, each determined as the respective excess water to solid surface area ratio, are tabulated in the last column of Table 1. For the mortar samples tested, the WFT ranged from −0·163 μm to 0·282 μm. It should be noted that a negative WFT value indicates that the amount of water in the mortar was not sufficient to fill the voids between the solid particles, leading to the entrapment of air in the mortar. To study the roles of the WFT, the fresh and hardened properties are correlated to the WFT by regression analysis, as presented in the following.

Effects of WFT on flow spread and flow rate

By plotting the flow spread against the WFT as shown in the upper half of Figure 7, it can be seen that regardless of the SFC and CSF contents, the flow spread increased with the WFT at a gradually decreasing rate. However, at the same WFT, a mortar with CSF added generally has a larger flow spread than a mortar with no CSF added. To study the combined effects of the WFT and CSF content, multi-variable regression analysis has been carried out to derive the best-fit curves for the flow spread–WFT relation. The best-fit curves so obtained are plotted alongside the data points and the equation and R^2 value are printed in the graph. The equation suggests that the maximum flow spread is

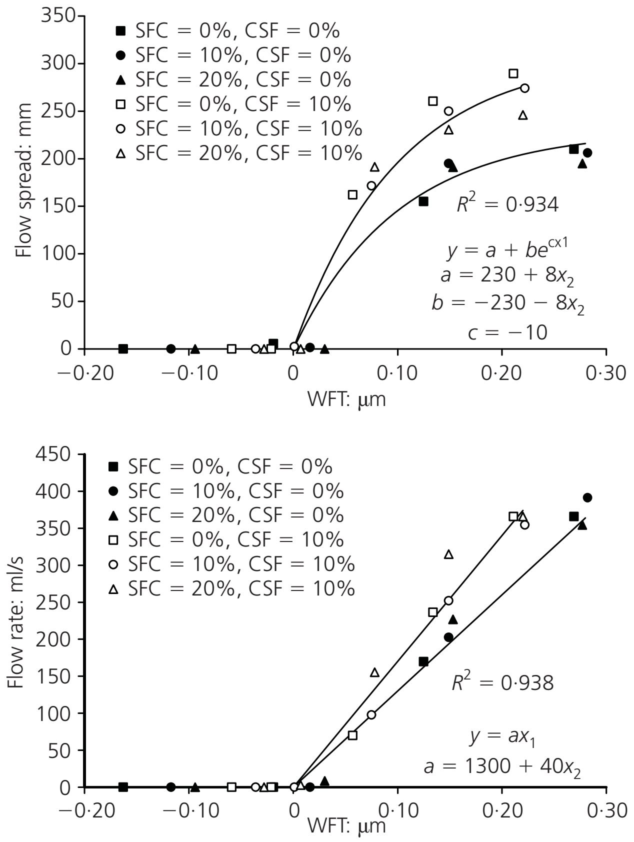

Figure 7. Flowability against WFT. Note: x_1 is the WFT (μm); x_2 is the CSF content (%)

larger when CSF is added. The very high R^2 value of 0·934 achieved with both the WFT and CSF content considered indicates that the flow spread is governed by both the WFT and CSF content.

By plotting the flow rate against the WFT as shown in the lower half of Figure 7, it can be seen that regardless of the SFC and CSF contents, the flow rate increased with the WFT at a more or less constant rate. However, at the same WFT, a mortar with CSF added generally has a higher flow rate than a mortar with no CSF added. To study the combined effects of the WFT and CSF content, multi-variable regression analysis has been carried out to derive the best-fit curves for the flow rate–WFT relation. As before, the best-fit curves so obtained are plotted alongside the data points and the equation and R^2 value are printed in the graph. The two best-fit curves plotted as straight lines reveal that the flow rate–WFT relation is basically linear. Furthermore, the very high R^2 value of 0·938 achieved reveals that the WFT and CSF content are the main factors governing the flow rate.

Overall, the effects of CSF are that at the same WFT, a mortar with CSF added has larger flow spread and higher flow rate than a mortar with no CSF added. Since the effects of CSF on the packing density and solid surface area should have been reflected in the WFT, it seems that the CSF has certain additional effects not reflected by the WFT. Such additional effects of CSF may be explained as follows. First, due to their high fineness, the CSF particles would tend to move together with the water to form a water–CSF slurry. Since the water–CSF slurry has a larger volume than the water itself, the presence of CSF would increase the thickness of slurry coating the cement and aggregate particles to provide better lubrication. Second, due to their perfectly rounded shape, the CSF particles could act as ball bearings to reduce the inter-particle friction between the cement and aggregate particles.

Effects of WFT on yield stress and apparent viscosity

The yield stress is plotted against the WFT in the upper half of Figure 8 to illustrate the effect of WFT on yield stress. In general, the yield stress decreased as the WFT increased. These results also reveal that the yield stress is governed not only by the WFT, but also by the CSF content. To study the combined effects of the WFT and CSF content, multi-variable regression analysis has been carried out to derive the best-fit curves for the yield stress–WFT relation. The best-fit curves so obtained are plotted alongside the data points and their equations and R^2 value are printed

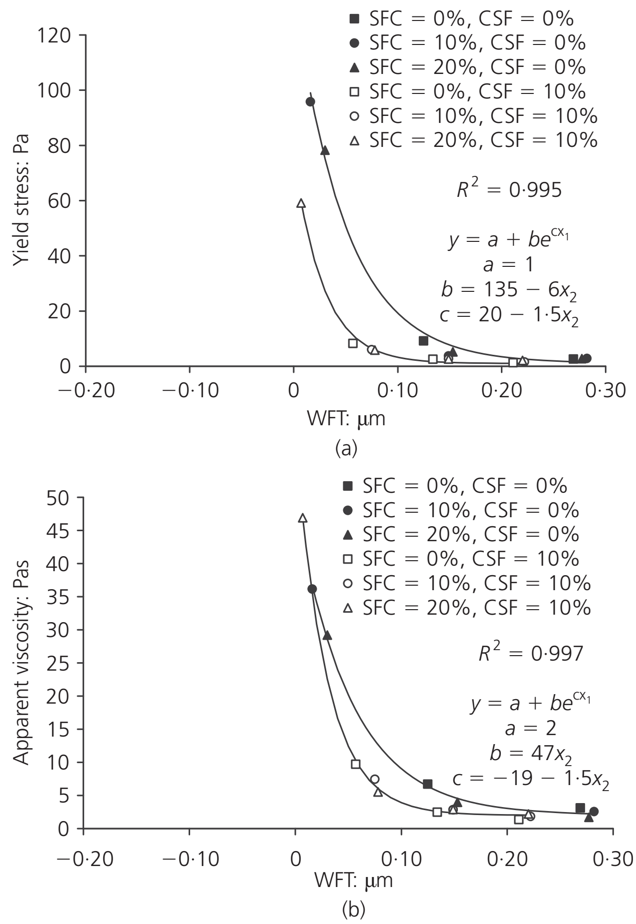

Figure 8. Rheological properties against WFT. Note: x_1 is the WFT (μm); x_2 is the CSF content (%)

in the graph. It is noted that with the addition of CSF, the best-fit curve shifts downwards and to the left. Such shifting suggests that at the same WFT, the presence of CSF would significantly decrease the yield stress. It is noteworthy that with both the WFT and CSF content considered in the correlation, the R^2 reaches a very high value of 0·995, indicating that the WFT and CSF content are the controlling factors governing the yield stress.

The apparent viscosity is plotted against the WFT in the lower half of Figure 8 to illustrate the effect of WFT on apparent viscosity. As for the yield stress, the apparent viscosity also decreased as the WFT increased. Moreover, the apparent viscosity is governed not only by the WFT, but also by the CSF content. To study the combined effects of the WFT and CSF content, multi-variable regression analysis has been carried out to derive the best-fit curves for the apparent viscosity–WFT relation. The best-fit curves so obtained and the equation and R^2 value are presented in the graph for easy reference. With CSF added, the best-fit curve shifts downwards and to the left. Such shifting reveals that at the same WFT, the addition of CSF would significantly decrease the apparent viscosity. A very high R^2 value of 0·997 has been achieved in the correlation, indicating that the apparent viscosity is dependent mainly on the WFT and CSF content.

The above results that both the yield stress and apparent viscosity decreased as the WFT increased are expected because a water–solid mixture with a larger WFT should have smaller yield stress and apparent viscosity. It is more interesting to note that the effects of CSF on the yield stress and apparent viscosity are similar to the effects of CSF on the flow spread and flow rate. An obvious reason is that the flow spread and flow rate are closely related to the yield stress and apparent viscosity, respectively (Kwan *et al.*, 2010; Tattersall and Banfill, 1983), and thus they should be similarly affected by the CSF.

Effect of WFT on adhesiveness

From the adhesiveness–WFT curves plotted in Figure 9, it can be seen that, compared to the W/S ratio, the WFT has a clearer effect on the adhesiveness of mortar. On the whole, when the WFT was negative, the mortar appeared to be rather dry and the adhesiveness was very small or zero. As the WFT increased, the mortar became slightly wetter and the adhesiveness increased dramatically to a certain maximum value. Then, as the WFT increased further, the mortar became quite wet and the adhesiveness decreased. Hence, for each combination of SFC and CSF contents, there was an optimum WFT at which the adhesiveness reached a certain maximum value. In general, the optimum WFT giving the maximum adhesiveness was around 0–0·10 μm. It may thus be said that the adhesiveness is highest when the mortar is neither too dry nor too wet, as indicated by its WFT, taken as a measure of wetness, falling within 0 to 0·10 μm. This is an important guideline for the design of high-build mortar for rendering and repair, and the mortar portion of high segregation stability concrete, which are required to have high adhesiveness.

Regarding the effects of SFC and CSF contents, the test results have not revealed any clear trend. Frankly speaking, the stepwise variations of the WFT were not small enough to yield all the sharp peaks in the adhesiveness–WFT curves. Hence, the maximum adhesiveness tended to be underestimated. Nevertheless, it does seem that the addition of SFC and/or CSF is beneficial to the adhesiveness; further tests are of course needed for confirmation.

Effect of WFT on cube strength

From the cube strength–WFT curves plotted in Figure 10, it can be seen that the WFT has a distinct effect on the strength of mortar. When the WFT was negative, the mortar appeared to be rather dry because the water was then not sufficient to fill the voids. Under this situation, a certain amount of air was entrapped in the voids causing the strength of mortar to be adversely affected. When the WFT was positive, the water was sufficient to fill the voids. Under this situation, as the WFT increased, the W/CM ratio also increased causing the strength of mortar to decrease gradually. Hence, the maximum strength was achieved at a WFT very close to 0 μm, in which case the water was just

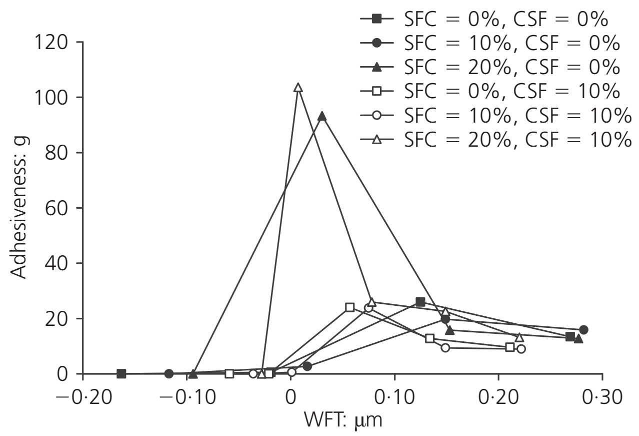

Figure 9. Adhesiveness against WFT

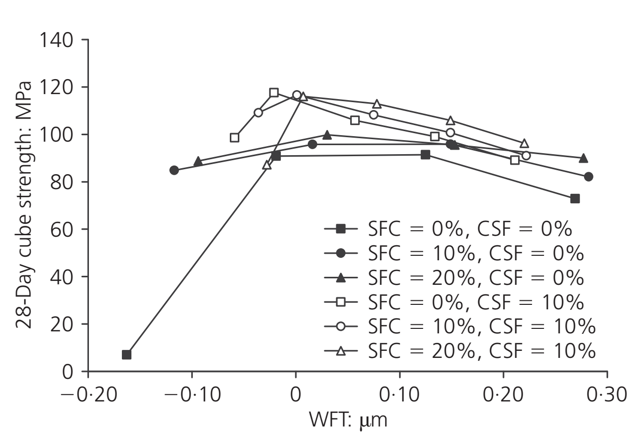

Figure 10. Cube strength against WFT

sufficient to fill the voids. As a general rule, therefore, to achieve the highest strength possible, a positive but very small WFT should be adopted in the design of the mortar mix.

Conclusions

A number of mortar samples made with triple-blended cementitious materials containing OPC + SFC + CSF and added with different water contents were produced for packing density, rheology, adhesiveness and strength measurements. It was found that the addition of SFC, which is finer than OPC, to fill the voids between OPC, and the addition of CSF, which has the highest fineness, to fill the voids between OPC and SFC can significantly increase the packing density of the solid particles. However, because of the respective increase in solid surface area, which thins down the water films coating the solid particles, the WFT does not always increase. Relatively, the addition of SFC is less effective in increasing the WFT but would increase the WFT over a wider range of water content, and the addition of CSF is more effective in increasing the WFT but would increase the WFT only at W/S ratio by volume $\leqslant$ 0·45 or W/CM ratio by mass $\leqslant$ 0·32.

Correlation of the measured flow spread, flow rate, yield stress, apparent viscosity and adhesiveness to the WFT revealed that the WFT plays an important role in the fresh properties of mortar. Generally, the flow spread and flow rate would increase and the yield stress and apparent viscosity would decrease as the WFT increases. At the same WFT, the SFC has little effect but the CSF has great effects on these rheological properties. This is probably because the CSF, being ultrafine, would tend to move together with the water to form a water–CSF slurry, which has a large volume than the water itself, to provide better lubrication; and the CSF, being perfectly rounded, could act as ball bearings to reduce the inter-particle friction between the larger solid particles. On the other hand, it is evident that the adhesiveness is highest when the mortar is neither too dry nor too wet, as indicated by its WFT, taken as a measure of wetness, falling within 0–0·10 μm.

Lastly, the strength results revealed that the WFT also plays an important role in the hardened properties of mortar. Basically, a positive but very small WFT is the optimum for producing the highest strength. Furthermore, the addition of SFC and/or CSF to increase the packing density would allow the W/CM ratio to be lowered while keeping the WFT positive to increase the strength.

Acknowledgement

The work described in this paper was fully supported by a GRF grant from the Research Grants Council of the Hong Kong Special Administrative Region, China (project no. 713309).

REFERENCES

Aïtcin P-C (1998) *High-Performance Concrete*. E & FN Spon, London, UK.

Artelt C and Garcia E (2008) Impact of superplasticizer concentration and of ultra-fine particles on the rheological behaviour of dense mortar suspensions. *Cement and Concrete Research* **38(5)**: 633–642.

ASTM (2003) C 1240-03. Standard specification for use of silica fume as a mineral admixture in hydraulic-cement conrete, mortar, and grout. McGraw-Hill, USA.

BSI (2000) BS EN 197-1: 2000. Cement. Composition, specifications and conformity criteria for common cements. BSI, London, UK.

BSI (2010) BS EN 196-6: 2010. Methods of testing cement. Determination of fineness. BSI, London, UK.

Claisse PA, Lorimer P and Al Omari M (2001) Workability of cement pastes. *ACI Materials Journal* **98(6)**: 476–482.

Duval R and Kadri EH (1998) Influence of silica fume on the workability and the compressive strength of high-performance concretes. *Cement and Concrete Research* **28(4)**: 533–547.

Ferraris CF, Obla KH and Hill R (2001) The influence of mineral admixtures on the rheology of cement paste and concrete. *Cement and Concrete Research* **31(2)**: 245–255.

FIP Commission on Concrete (1988) *Condensed Silica Fume in Concrete*. FIP State of the Art Report, Thomas Telford, London, UK.

Fung WWS, Kwan AKH and Wong HHC (2009) Wet packing of crushed rock fine aggregate. *Materials and Structures* **42(5)**: 631–643.

Helmuth RA (1980) Structure and rheology of fresh cement paste. *Proceedings of 7th International Congress of Chemistry of Cement, Paris, France*, pp. 16–30.

Khatri RP, Sirivivatnanon V and Gross W (1995) Effect of different supplementary cementitious materials on mechanical properties of high performance concrete. *Cement and Concrete Research* **25(1)**: 209–220.

Kohno K and Komatsu H (1986) Use of ground bottom ash and silica fume in mortar and concrete. *Proceedings of Second International Conference on Fly Ash, Silica Fume, Slag, and Natural Pozzolans in Concrete, Madrid, Spain*, pp. 1279–1292.

Kwan AKH (2003) Development of high performance concrete for Hong Kong. *Proceedings of Materials Science and Technology in Engineering Conference, Hong Kong*, pp. 1–16.

Kwan AKH and Fung WWS (2009) Packing density measurement and modelling of fine aggregate and mortar. *Cement and Concrete Composites* **31(6)**: 349–357.

Kwan AKH and Wong HHC (2008) Effects of packing density, excess water and solid surface area on flowability of cement paste. *Advances in Cement Research* **20(1)**: 1–11.

Kwan AKH, Fung WWS and Wong HHC (2010) Water film thickness, flowability and rheology of cement-sand mortar. *Advances in Cement Research* **22(1)**: 3–14.

Kwan AKH, Chen JJ and Fung WWS (2012) Effects of superplasticizer on rheology and cohesiveness of CSF cement paste. *Advances in Cement Research* **24(3)**: 125–137.

Okamura H and Ouchi M (2003) Self-compacting concrete. *Journal of Advanced Concrete Technology* **1(1)**: 5–15.

Powers TC (1968) *The Properties of Fresh Concrete*. Wiley, New York, USA.

Rizwan SA and Bier TA (2009) Self-consolidating mortars using various secondary raw materials. *ACI Materials Journal* **106(1)**: 25–32.

Svarovsky L (1987) *Powder Testing Guide: Methods of Measuring the Physical Properties of Bulk Powders*. Elsevier Applied Science, UK.

Tattersall GH and Banfill PFG (1983) *The Rheology of Fresh Concrete*. Pitman, Boston, USA.

Wong HHC and Kwan AKH (2008a) Rheology of cement paste: role of excess water to solid surface area ratio. *Journal of Materials in Civil Engineering* **20(2)**: 189–197.

Wong HHC and Kwan AKH (2008b) Packing density of cementitious materials: Part 1 – measurement using a wet packing method. *Materials and Structures* **41(4)**: 689–701.

Wong HHC and Kwan AKH (2008c) Packing density of cementitious materials: measurement and modelling. *Magazine of Concrete Research* **60(3)**: 165–175.

Yu AB, Bridgwater J and Burbidge A (1997) On the modelling of the packing of fine particles. *Powder Technology* **92(3)**: 185–194.

Zhang C, Wang A, Tang M and Liu X (1996) The filling role of pozzolanic material. *Cement and Concrete Research* **26(6)**: 943–947.

Zhang X and Han J (2000) The effect of ultra-fine admixture on the rheological property of cement paste. *Cement and Concrete Research* **30(5)**: 827–830.

WHAT DO YOU THINK?

To discuss this paper, please submit up to 500 words to the editor at www.editorialmanager.com/acr by 1 August 2013. Your contribution will be forwarded to the author(s) for a reply and, if considered appropriate by the editorial panel, will be published as a discussion in a future issue of the journal.